Received: 28 March 2023 | Accepted: 22 April 2023

DOI: 10.1111/1759-7714.14926

ORIGINAL ARTICLE

WILEY

Exosomal ERBB2IP contributes to tumor growth via elevating PSAT1 expression in non-small cell lung carcinoma

Xijuan Peng[1] | Lanfu Zhao[2] | Linong Yao[1] | Jingzhi Dong[1] | Wei Wu[1] | Tao Luo[2]

[1]Department of Critical Medicine, The Second Affiliated Hospital of Air Force Medical University, Xi'an, China

[2]Department of Neurosurgery, The Second Affiliated Hospital of Air Force Medical University, Xi'an, China

Correspondence
Tao Luo, Department of Neurosurgery, The Second Affiliated Hospital of Air Force Medical University, No.1, Xinsi Road, Baqiao District, Xi'an, Shaanxi, China, 710038.
Email: 1982101119@163.com

Abstract

Background: Both exosomes and circular RNAs (circRNAs) are involved in tumor growth. Hsa_circ_0001492 (circERBB2IP) has been reported to be overexpressed in plasma exosomes from patients with lung adenocarcinoma, but the biological role of exosomal circERBB2IP in non-small cell lung carcinoma (NSCLC) is indistinct.

Methods: Exosomes isolated from serums and medium samples were validated by transmission electron microscopy (TEM), nanoparticle tracking analysis (NTA), and western blotting. Relative expression of circERBB2IP was detected by RT-qPCR. Loss-of-function was done to determine the effect of circERBB2IP on NSCLC cell proliferation and migration. Molecular mechanisms associated with circERBB2IP were predicted by bioinformatic analysis and validated by dual-luciferase reporter, RIP, and RNA pulldown assays. In vivo experiments were performed to identify the function of circERBB2IP in NSCLC.

Results: We discovered that circERBB2IP expression was correlated with TNM grade, lymph node metastasis and tumor size of NSCLC patients. Upregulation of circERBB2IP was observed in exosomes derived from NSCLC patient's serum and circERBB2IP might be a potential diagnostic biomarker for NSCLC. CircERBB2IP was transmitted between carcinoma cells through exosomes. Knockdown of circERBB2IP lowered cell growth in mouse models and restrained NSCLC cell proliferation and migration. CircERBB2IP could mediate PSAT1 expression via sponging miR-5195-3p.

Conclusion: In conclusion, circERBB2IP may drive NSCLC growth by the miR-5195-3p/PSAT1 axis in NSCLC, shedding light on a diagnostic biomarker and therapeutic target for NSCLC.

KEYWORDS
circERBB2IP, exosomes, miR-5195-3p, NSCLC, PSAT1

INTRODUCTION

The most malignant subtype of lung carcinoma is non-small cell lung carcinoma (NSCLC).[1] A large proportion of patients have already developed mediastinal lymph node metastasis at the time of diagnosis. The long-term survival rate of patients with advanced lung carcinoma is still very poor that targeted therapy and immunotherapy have made progress.[2,3] Therefore, exploring new mechanisms to promote NSCLC progression is crucial.

Circular RNAs (circRNAs) have a closed-loop structure, which gives them high stability. These closed circular transcripts are made by reverse splicing rather than classical splicing. Recent studies have shown the contribution of circular RNAs in the physiological environment, development process, and pathological mechanism of carcinoma.[4] For instance, circPLCE1 curbs colorectal carcinoma progression via disrupting NF-κB nuclear translocation.[5] CircEYA3 also

Xijuan Peng and Lanfu Zhao contributed equally to this work.

This is an open access article under the terms of the Creative Commons Attribution-NonCommercial-NoDerivs License, which permits use and distribution in any medium, provided the original work is properly cited, the use is non-commercial and no modifications or adaptations are made.
© 2023 The Authors. *Thoracic Cancer* published by China Lung Oncology Group and John Wiley & Sons Australia, Ltd.

contributes to pancreatic ductal adenocarcinoma progression by elevating energy production.[6] Gathering evidence reveals the vital role of circRNAs in NSCLC progression.[7] For instance, circIGF2BP3 facilitates carcinoma cell immune evasion in NSCLC.[8] CircCUL2 plays a promoting effect on NSCLC cell epithelial-mesenchymal transition (EMT).[9] Hsa_circ_0001492, also known as circERBB2IP, is derived from the ERBB2IP gene. It was previously reported that circERBB2IP promotes carcinoma cell metastasis and growth in colorectal carcinoma by activating HIF-1α.[10] Also, circERBB2IP has been discovered to be overexpressed in plasma exosomes from lung adenocarcinoma patients.[11]

Exosomes, which are extracellular vesicles with a diameter of 30–150 nm, are packed with a variety of molecules, such as steroids, hormones, carbohydrates, immune components, RNA, and lipids.[12] Exosomes participate in cell-to-cell communication to initiate or inhibit various signaling pathways in recipient cells by transmitting heterogeneous cargoes.[13] Moreover, exosomes have become potential regulators of intracellular communication in carcinoma.[14] However, the function of exosomal circERBB2IP has not been elucidated in NSCLC.

The identification of circRNAs as important regulators of microRNA (miRNA) activity underscores the increasing complexity of circRNA-mediated regulatory networks.[15] Through bioinformatic analysis, we found that circERBB2IP might be a sponge of miR-5195-3p. A series of reports manifests the suppressive effect of miR-5195-3p in human tumors.[16–19] PSAT1, a member of the Class V pyridoxal phospho-dependent aminotransferase family, participates in the serine synthesis pathway, which is a glycolytic shunt that is responsible for the conversion of 3-phosphoglycerate to serine through a series of reactions.[20] The oncogenic role of PSAT1 has been demonstrated in diverse carcinomas, such as ER-negative breast carcinoma,[21] ovarian carcinoma,[22] colorectal carcinoma,[23] and lung carcinoma.[24,25] However, the network mechanisms among circERBB2IP, miR-5195-3p, and PSAT1 are indistinct.

In this study, we hypothesized that exosomal circERBB2IP participated in NSCLC cell malignant phenotypes. Furthermore, we investigated whether circERBB2IP mediated NSCLC cell malignant phenotypes via the miR-5195-3p/PSAT1 axis.

METHODS

Study subjects

In total, 56 patients with NSCLC who underwent surgery at the Second Affiliated Hospital of Air Force Medical University were recruited to the study. Blood samples (56 NSCLC cases and 56 controls) were collected in EDTA-coated collection tubes. Patient characteristics are summarized in Table 1. The collected blood samples were clotted for about 30 min at room temperature, followed by centrifugation at 1500*g* for 10 min to obtain serum. The permission for this study was granted by the Ethical Committee of the Second Affiliated Hospital of Air Force Medical University.

TABLE 1 Relationship between circERBB2IP expression and clinicopathological features of NSCLC patients.

		circERBB2IP expression		
	Characteristics $n = 56$	**Low** ($n = 28$)	**High** ($n = 28$)	***p*-value**
Gender				0.7875
Female	24	13	11	
Male	32	15	17	
Age (years)				>0.9999
≤60	25	12	13	
>60	31	16	15	
TNM grade				0.0029*
I + II	26	19	7	
III + IV	30	9	21	
Lymph node metastasis				0.0026*
Positive	32	10	22	
Negative	24	18	6	
Tumor size				0.0069*
≤3 cm	29	20	9	
>3 cm	27	8	19	

Abbreviation: NSCLC, non-small cell lung cancer: TNM, tumor-node-metastasis.
*$p < 0.05$.

Preparation of exosomes

After filtration with a 0.45 μm polyvinylidene fluoride filter (Millipore, Germany), the serum and medium samples were supplemented with ExoQuick solution (System Biosciences, USA) and ExoQuick-TC solution (System Biosciences), respectively. The serum samples were incubated at room temperature for 30 min, but the medium samples were incubated at 4°C for 12 h. Then, these samples were centrifuged (1500*g*, 30 min), followed by collecting the exosomal particles and resuspending them in phosphate-buffered saline (PBS) (Thermo Fisher).

Identification of exosomes

The morphology of the isolated exosomes was visualized using a transmission electron microscope (TEM) (JEM-2100; JEOL) as previously described.[26] The concentration and diameter distribution of the isolated exosomes were analyzed using a NanoSight LM10 system (NanoSight) with the nanoparticle tracking analysis (NTA) 2.3 analytical software (NanoSight). Exosomal surface markers, such as CD63, CD81, and TSG101 were analyzed by western blotting.

Cell culture

NSCLC cells A549 (ZQ0003, Zhong Qiao Xin Zhou Biotechnology Co., Ltd.) and H1299 (ZQ0007) were cultured

in their respective complete medium, the product numbers were ZQ-509 and ZQ-201. The BEAS-2B cell line (ZQ0381) was cultured in its dedicated complete medium (ZQ-1313).

Plasmids, oligonucleotides, and cell transfection

The pLKO.1 (Addgene) recombinant plasmid carrying si-circERBB2IP (sh-circERBB2IP) or control (sh-NC) was constructed, and lentiviral particles carrying sh-circERBB2IP or sh-NC were used to infect A549 and H1299 cell lines to produce stable circERBB2IP knockdown NSCLC cells. The pcDNA (Addgene) recombinant plasmid carrying PSAT1 (PSAT1) was constructed for overexpression of PSAT1. miR-5195-3p inhibitor (in-miR-5195-3p, miR-5195-3p mimic [miR-5195-3p]), and their negative controls in-miR-NC and miR-NC were synthesized by Ribobio. Transfection was executed using lipofectamine RNAiMax (Thermo Fisher) or lipofectamine 3000 (Thermo Fisher) with Opti-MEM medium (Thermo Fisher).

Real-time quantitative polymerase chain reaction (RT-qPCR)

Isolation of total RNA from preisolated exosomes and NSCLC cells was performed using the exosomal RNA isolation kit (Norgren) or PicoPure RNA isolation kit (Thermo Fisher). The synthesis of complementary DNA from total RNA (400 ng) was performed using the M-MLV reverse transcriptase kit (Promega) or miScript II RT kit (Qiagen). RT[27] SYBR Green qPCR Master Mix (Qiagen) or miRCURY LNA SYBR Green PCR Kit (Qiagen) and specific primers (Table 2) for circERBB2IP, miR-5195-3p, and PSAT1 were used for quantitative PCR analysis in triplicate. The fold change in circERBB2IP, miR-5195-3p, and PSAT1 expression was calculated by the equation $2^{-\Delta\Delta Ct}$, and the housekeeping genes β-actin and U6 were used for normalization.

TABLE 2 Primer sequences used for real-time quantitative polymerase chain reaction (RT-qPCR).

Name		Primers for qRT-PCR (5′-3′)
circERBB2IP	Forward	TACCAGCATCCATTGCAAAC
	Reverse	ACCAACCGCACAAACAAACT
miR-5195-3p	Forward	GCGCGATCCAGTTCTCTGAG
	Reverse	AGTGCAGGGTCCGAGGTATT
PSAT1	Forward	AAAAACAATGGAGGTGCCGC
	Reverse	GGCTCCACTGGACAAACGTA
U6	Forward	CTCGCTTCGGCAGCACATA
	Reverse	CGAATTTGCGTGTCATCCT
β-actin	Forward	CAGCCATGTACGTTGCTATCCA
	Reverse	TCACCGGAGTCCATCACGAT

3-(4,5-dimethylthiazol-2-yl)-2,5-diphenyltetrazolium bromide (MTT) assay

NSCLC cells (4000 cells/well) are cultured in 96-well plates. After 24, 48, or 72 h of incubation, 5 μL of MTT solution (5 mg/mL, Sigma) was added to each well and incubated for 1 h. After aspirating the medium, 100 μL of DMSO (Sigma) was added to dissolve the crystals. Analysis of the absorbance of the solution was performed on an automatic enzyme-linked immunosorbent assay reader (BioTek) at 490 nm. Each experiment (in triplicate) was repeated three times to assess the consistency of the results.

5-ethynyl-2′-deoxyuridine (EdU) assay

The Yefluor 594 EdU imaging kit (red fluorescence) (Yeasen) was used for analysis of cell proliferation on the basis of the manufacturer's instructions. Nuclear counterstain was performed using DAPI (Yeasen). A fluorescence microscope (Olympus) was used to capture images.

Transwell migration and invasion assays

Transwell chambers (6.5-mm in diameter: Corning), with or without matrigel, were used for invasion and migration analysis. Cells were added to the upper chamber and suspended in 200 μL of medium containing 0.5% bovine serum albumin (Yeasen), and 500 μL of complete medium was added to the lower chamber. After 24 h of incubation, the migrating and invading cells were fixed with 4% paraformaldehyde (Sangon) and then stained with 0.1% crystal violet (Sangon). Images were taken under a microscope (Olympus).

Western blotting

A total exosome RNA and protein isolation kit (Thermo Fisher) was utilized to extract protein from exosomes. Radioimmunoprecipitation (RIPA) lysis buffer was employed to lyse the culture cells, and the total protein was then collected. Protein samples were denatured and subjected to SDS-PAGE electrophoresis, followed by electrophoresis on a nitrocellulose membrane (Boster) and immersed in 5% skimmed milk. The membranes were probed with primary antibodies, including anti-E-cad (#14472, Cell Signaling), anti-N-cad (#14215, Cell Signaling), anti-vimentin (#3390, Cell Signaling), and anti-PSAT1 (#67619-1-Ig, Proteintech), anti-CD63 (#67605-1-Ig, Proteintech), anti-CD81 (#66866-1-Ig, Proteintech), anti-TSG101 (#67381-1-Ig, Proteintech), and anti-β-actin (#3700, Cell Signaling) antibodies. After incubation with a secondary antibody, the bands were visualized using chemiluminescence (Thermo Fisher).

Dual-luciferase reporter assay

The pMIR-REPORT (Promega) recombinant plasmid carrying circERBB2IP-WT, circERBB2IP-MUT, PSAT1 3'UTR-WT, or PSAT1 3'UTR-MUT were constructed, respectively. NSCLC cells were cotransfected with pRL-TK, recombinant plasmid, and miR-5195-3p mimic or miR-NC using lipofectamine RNAiMAX reagent (Thermo Fisher). Luciferase activities were analyzed with a dual-luciferase reporter assay kit (Promega) on a varioskan LUX microplate reader (Thermo Fisher).

RNA immunoprecipitation (RIP) assay

A Magna RIP RNA-binding protein immunoprecipitation kit (Millipore) was utilized to evaluate the involvement of circERBB2IP and miR-5195-3p following the manufacturer's guidelines. Briefly, NSCLC cells were lysed. And the collected supernatants were incubated with magnetic beads conjugated with an antibody against IgG (Millipore) or Ago2 (Millipore). The immunoprecipitated RNAs were extracted and then purified for RT-qPCR analysis.

RNA pulldown assay

The NSCLC cells transfected with Bio-miR-NC, Bio-miR-5195-3p MUT, Bio-miR-5195-3p WT were lysed. The collected supernatants were incubated with activated M-280 streptavidin beads (Sigma) at 4°C. The RNA complexes bound to the beads were eluted for RT-qPCR analysis.

In vivo experiments

The permission for in vivo experiments was granted by the Animal Ethics Committee of the Second Affiliated Hospital of Air Force Medical University. Ten nude mice (BALB/c, 4-week-old) (Vital River, Beijing, China) were fed in a specific pathogen-free environment. After 1 week of acclimatization, the mice were injected with A549 cells with sh-NC or sh-circERBB2IP. Tumor volume was measured once a week (volume = [length × width^2]/2). The mice were sacrificed after 4 weeks of injection. The tumors were collected for weight assessment and immunohistochemistry (IHC) analysis.

IHC analysis

Xenograft tissues were fixed in formalin and then dehydrated and embedded in paraffin. Then, the tissue sections were incubated with an antibody against PSAT1 (no. 67619-1-Ig, Proteintech), Ki67 (no. 9449, Cell Signaling), E-cad (no. 14472, Cell Signaling), N-cad (no. 13116, Cell Signaling), or vimentin (no. 5741, Cell Signaling) overnight. After washing, the sections were incubated with a secondary antibody coupled with horseradish peroxidase. IHC images were observed under a microscope (Olympus).

Statistical analysis

Data analysis and graphical presentations were performed using SPSS version 20.0 (SPSS Inc., USA) and GraphPad Prism 8 (GraphPad Software, Inc., USA). Significance was determined using Student's *t*-test for pairwise comparison or analysis of variance with Tukey's test for multiple comparisons. p-values < 0.05 indicated statistical significance.

RESULTS

Serum-derived exosomal circERBB2IP acted as potential diagnostic biomarker for NSCLC

In this study, we first detected circERBB2IP expression in 56 NSCLC samples. We discovered that circERBB2IP expression was correlated with TNM grade, lymph node metastasis and tumor size of NSCLC patients (Table 1). Subsequently, we isolated exosomes from collected serum samples. TEM images showed the characteristic exosomal saucer-shaped morphology typical of isolated vesicles (Figure 1a). Nanoparticle tracking analysis (NTA) showed that the size of the isolated vesicles ranged from 30 to 150 nm, which was consistent with the expected size range (Figure 1b). Subsequently, the isolated vesicles were confirmed to be exosomes by detecting the exosomal markers CD63, CD81, and TSG101 (Figure 1c). We then detected circERBB2IP levels in exosomes derived from serum samples of NSCLC patients and normal controls. Exosomes derived from patient serum expressed more circERBB2IP than exosomes derived from control serum (Figure 1d). Furthermore, the area under the curve (AUC) for exosomal circERBB2IP was 0.9168, indicating the diagnostic capacity of serum-derived exosomal circERBB2IP (Figure 1e). CircERBB2IP expression was consistently higher in NSCLC samples than those of normal samples (Figure 1f). Overall, exosomal circERBB2IP might be a diagnostic biomarker for NSCLC.

NSCLC cells can communicate through exosomal circERBB2IP in vitro

Based on the important role of exosomes in cell-to-cell communication, we further analyzed whether NSCLC cells can communicate through exosomal circERBB2IP. An increase in circERBB2IP expression was observed in NSCLC cell lines when compared with the BEAS-2B cell line (Figure 2a). Similarly, circERBB2IP was overexpressed in exosomes derived from NSCLC cells compared with exosomes derived from BEAS-2B cells (Figure 2b). Furthermore, circERBB2IP was lowly expressed in sh-circERBB2IP-transfected NSCLC cells

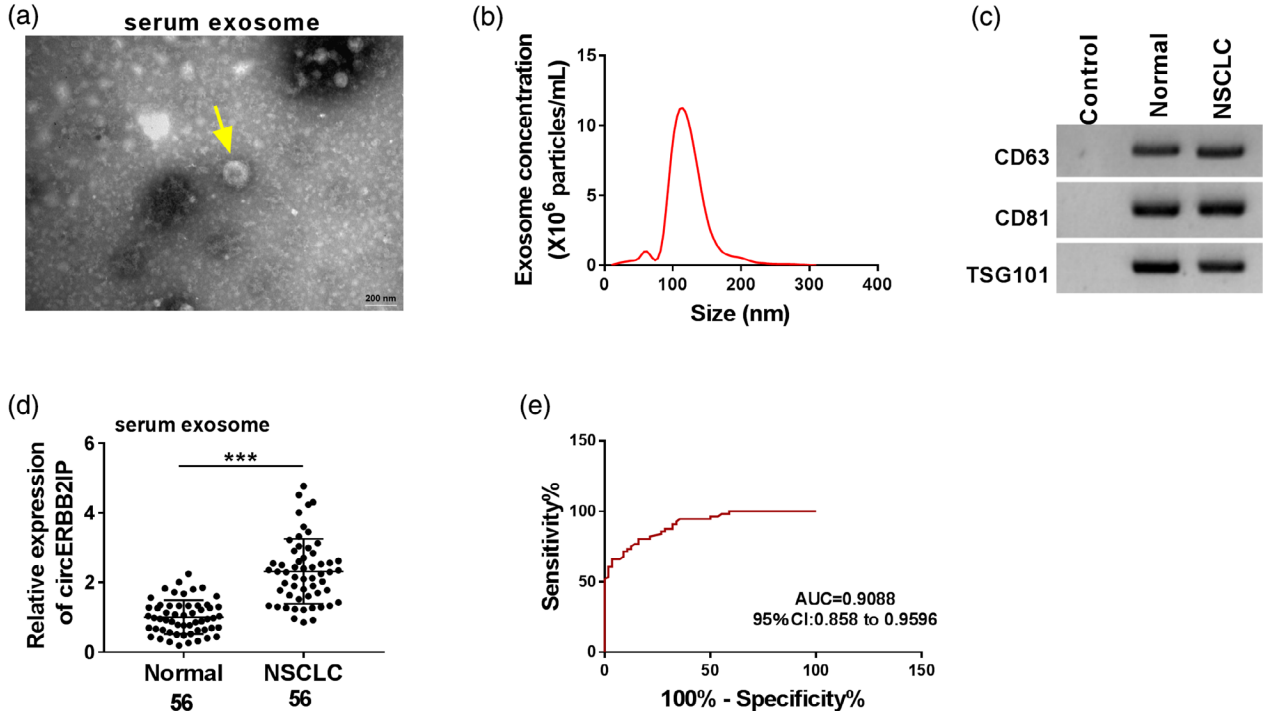

FIGURE 1 Characterization of human serum-derived exosomes. (a) Transmission electron microscopy (TEM) images of exosomes isolated from serum samples. (b) Nanoparticle tracking analysis (NTA) analysis of the particle size and concentration of the isolated exosomes. (c) Western blotting showing the detected exosomal markers CD63, CD81, and TSG101. (d) RT-qPCR exhibiting circERBB2IP levels in exosomes derived from serum samples of non-small cell lung cancer (NSCLC) patients and normal controls. (e) The receiver-operating characteristic (ROC) curve of exosomal circERBB2IP. (f) RT-qPCR analysis of circERBB2IP expression in NSCLC samples and normal samples. ***$p < 0.001$.

(Figure 2c). Consistently, the exosomes derived from sh-circERBB2IP-transfected NSCLC cells expressed less circERBB2IP than exosomes derived from sh-NC-transfected NSCLC cells (Figure 2d). We then detected circERBB2IP expression in NSCLC cells coincubated with PBS, cell exosomes, cell-sh-NC exosomes, or cell-sh-circERBB2IP exosomes. Data in Figure 2e exhibited that circERBB2IP expression was increased in NSCLC cells co-incubated with exosomes, but this increase was weakened after exosomal circERBB2IP knockdown. Interestingly, after treatment with exosomes inhibitors (GW4896), the level of circERBB2IP in the culture medium used for cultivating NSCLC cells was lower (Figure 2f). Overall, tumor cells can communicate through exosomal circERBB2IP in NSCLC.

CircERBB2IP knockdown decreased NSCLC cell malignant phenotypes

The effects of circERBB2IP on malignant phenotypes were then determined by loss-of-function experiments. Results of MTT and EdU assays exhibited that circERBB2IP knockdown restrained NSCLC cell proliferation (Figure 3a-d). Transwell assays showed that circERBB2IP silencing resulted in lower migration and invasion capabilities of NSCLC cells (Figure 3e, f). Furthermore, circERBB2IP downregulation increased E-cad protein levels and decreased N-cad and vimentin protein in NSCLC cells (Figure 3g, h). Collectively, circERBB2IP inhibition reduced NSCLC cell malignant phenotypes.

CircERBB2IP negatively regulated miR-5195-3p expression

To better understand the mechanism of circERBB2IP in NSCLC, we overlapped predicted miRNAs that might interact with circERBB2IP in 2 public databases (starBase and circBank). miR-5195-3p was then selected for further analysis (Figure 4a). After miR-5195-3p mimic transfection, miR-5195-3p was distinctly upregulated in NSCLC cells (Figure 4b). Luciferase activity assays showed that miR-5195-3p overexpression restrained the luciferase activity of the circERBB2IP-WT reporter, whereas no changes were noticed in the circERBB2IP-MUT reporter (Figure 4c, d). Anti-Ago2 RIP experiments presented that circERBB2IP and miR-5195-3p could be coenriched in the complex precipitated by the anti-Ago2 antibody (Figure 4e, f). RNA pull-down assay showed that the abundance of circERBB2IP was overtly higher in the complex pulled down by the Bio-miR-5195-3p WT probe but not the control probe (Figure 4g). Lower levels of miR-5195-3p were observed in NSCLC samples than in normal samples, and were negatively correlated with circERBB2IP (Figure 4h,i). As expected, miR-5195-3p expression was lower in NSCLC cells than the control cells

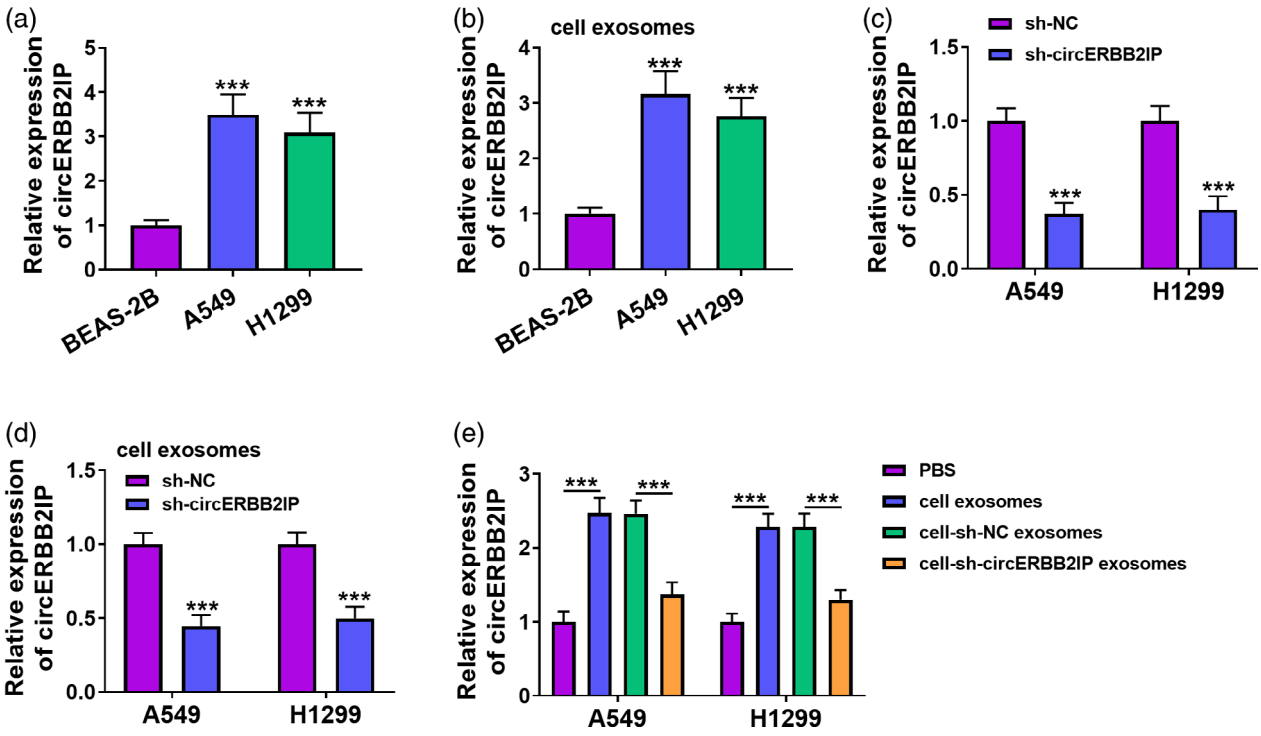

FIGURE 2 CircERBB2IP was transmitted between carcinoma cells through exosomes. (a-d) Relative levels of circERBB2IP in non-small cell lung cancer (NSCLC) cell lines (a), exosomes derived from NSCLC cells (b), NSCLC cell lines with sh-NC or sh-circERBB2IP (c), and exosomes derived from NSCLC cells with sh-NC or sh-circERBB2IP (d) were detected. (e) After co-incubation with PBS, cell exosomes, cell-sh-NC exosomes, or cell-sh-circERBB2IP exosomes, circERBB2IP expression in NSCLC cell lines were determined. (f) Relative levels of circERBB2IP in the culture medium supplemented with DMSO or GW4869, and the culture medium was used for cultivating NSCLC cells. ***$p < 0.001$.

(Figure 4j). Similarly, miR-5195-3p expression was significantly lower in exosomes from A549 and H1299 cells than those from BEAS-2B cells (Figure S1). Together, circERBB2IP served as a miR-5195-3p sponge.

CircERBB2IP mediated NSCLC cell malignant phenotypes via miR-5195-3p

We next investigated whether circERBB2IP participated in NSCLC cell malignant phenotypes through regulation of miR-5195-3p. The interference efficiency of miR-5195-3p inhibitor was confirmed and showed in Figure 5a. Moreover, miR-5195-3p knockdown crippled circERBB2IP silencing-mediated repression on NSCLC cell proliferation, migration, and invasion (Figure 5b-f). In addition, circERBB2IP downregulation-mediated effects on E-cad, N-cad, and vimentin protein levels were partly overturned after miR-5195-3p inhibition (Figure 5g). Overall, circERBB2IP modulated NSCLC cell malignant phenotypes through miR-5195-3p.

MiR-5195-3p negatively regulated PSAT1 expression

To further elucidate the targets of miR-5195-3p, Bioinformatic analysis was conducted by using starBase. We discovered that the binding sites of miR-5195-3p seed sequence were present in the 3'UTR of PSAT1 (Figure 6a). Data in Figure 6b, c displayed that miR-5195-3p upregulation caused a reduction in the luciferase activity of the PSAT1 3'UTR-MUT reporter. Overexpression of PSAT1 mRNA was detected in NSCLC samples relative to normal samples, and had a negative correlation with miR-5195-3p in NSCLC samples (Figure 6d, e). We also observed a marked elevation in PSAT1 mRNA and protein levels in NSCLC cells (Figure 6f, g). Moreover, miR-5195-3p mimic markedly reduced PSAT1 mRNA and protein levels in NSCLC cells (Figure 6h, i). Additionally, miR-5195-3p knockdown weakened circERBB2IP silencing-mediated inhibition on PSAT1 mRNA and protein levels in NSCLC cells (Figure 6j, k). Together, miR-5195-3p directly targeted PSAT1 in NSCLC cells.

CircERBB2IP regulated NSCLC cell malignant phenotypes through PSAT1

Considering circERBB2IP could modulate PSAT1 expression, we probed into whether PSAT1 was involved in NSCLC cell malignant phenotypes mediated by circERBB2IP. The transfection efficiency of the PSAT1 overexpression plasmid was displayed in Figure 7a. Moreover, PSAT1 overexpression partially offset the inhibitory effects of circERBB2IP downregulation on NSCLC cell proliferation, migration, and invasion (Figure 7b-f). Also, the changes in E-cad, N-cad, and vimentin protein

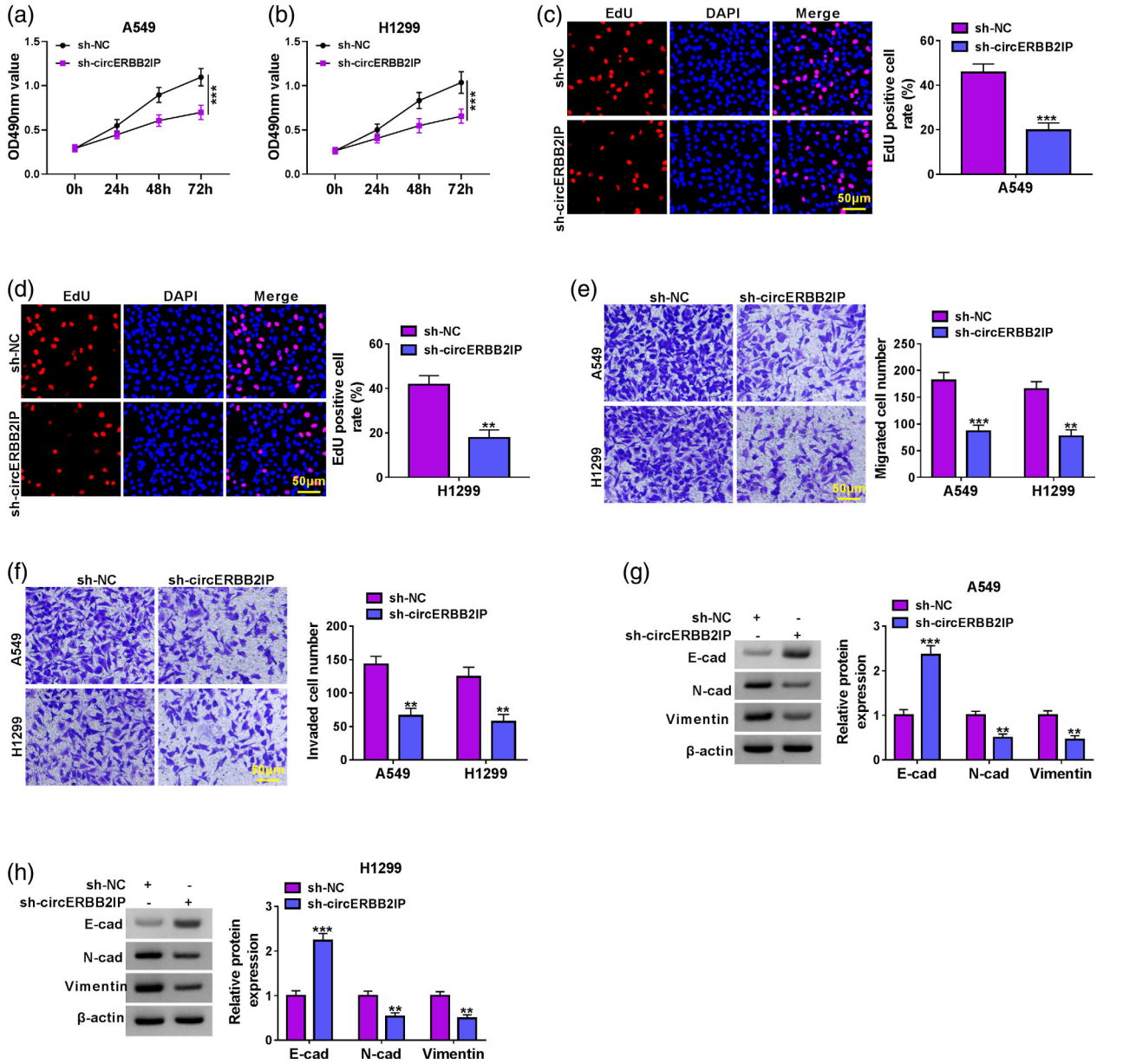

FIGURE 3 Effects of circERBB2IP inhibition on non-small cell lung cancer (NSCLC) cell malignant phenotypes. (a–f) Cell proliferation, migration, and invasion was determined by MTT (a and b), 5-ethynyl-2′-deoxyuridine (EdU) (c and d), and transwell assays (e and f) in NSCLC cell lines with sh-NC or sh-circERBB2IP. (g and h) Detection of E-cad, N-cad, and vimentin protein levels in NSCLC cell lines with sh-NC or sh-circERBB2IP. $^{**}p < 0.01$ and $^{***}p < 0.001$.

levels in circERBB2IP-silenced NSCLC cells were attenuated after PSAT1 introduction (Figure 7g, h). Overall, circERBB2IP regulated NSCLC cell malignant phenotypes through mediating PSAT1 expression.

CircERBB2IP inhibition reduced tumor growth in xenograft NSCLC mouse model NSCLC

We next conducted an in vivo study to verify the function of circERBB2IP in NSCLC. The tumors formed by A549 cells with sh-circERBB2IP in nude mice were smaller and lighter than tumors formed by A549 cells with sh-NC (Figure 8a, b). Furthermore, tumors formed by A549 cells with sh-circERBB2IP had lower levels of circERBB2IP and higher levels of miR-5195-3p compared with control tumors (Figure 8c). Tumors with circERBB2IP knockdown had significantly lower N-cad and vimentin protein levels and higher E-cad protein levels than control tumors (Figure 8d). Moreover, tumors formed by A549 cells with sh-circERBB2IP had fewer PSAT1/Ki67/N-cad/Vimentin-positive cells but more E-cad-positive cells (Figure 8e). Together, circERBB2IP inhibition reduced NSCLC cell growth in vivo.

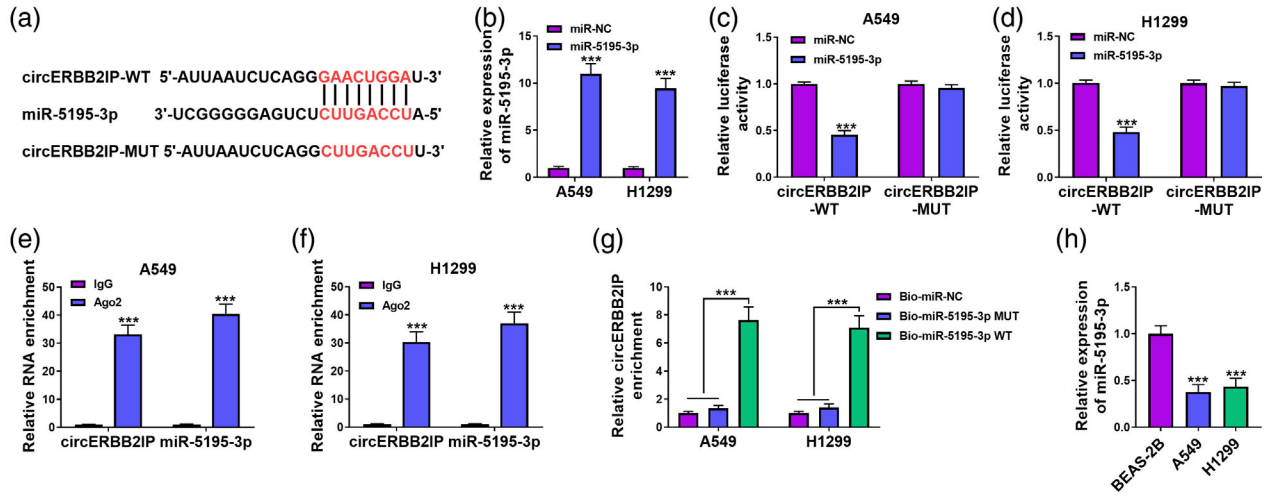

FIGURE 4 CircERBB2IP negatively regulated miR-5195-3p by acting as a miR-5195-3p sponge. (a) The predicted core binding sequence of miR-5195-3p in circERBB2IP sequence. (b) Relative levels of miR-5195-3p in NSCLC cell lines with miR-NC or miR-5195-3p. (c–g) The targeting relationship between circERBB2IP and miR-5195-3p was validated by luciferase assay (c and d), anti-Ago2 radioimmunoprecipitation (RIP) assay (e and f), and RNA pulldown assay (g). (h) Detection of miR-5195-3p expression in non-small cell lung cancer (NSCLC) samples and normal samples. (i) Pearson's correlation analysis was used to determine the correlation between miR-5195-3p and circERBB2IP expression levels in NSCLC samples. (j) Relative levels of miR-5195-3p in NSCLC cell lines. ***$p < 0.001$.

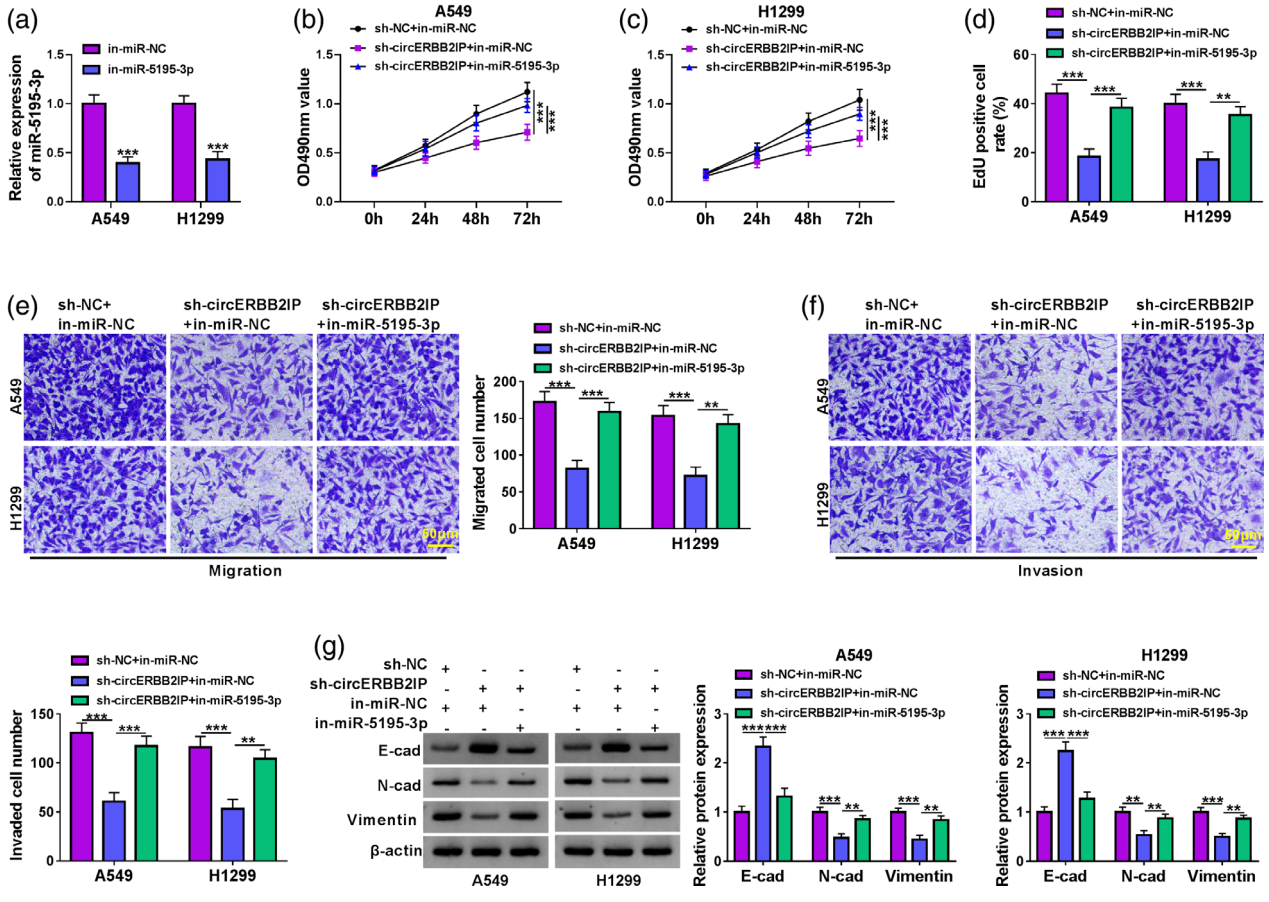

FIGURE 5 CircERBB2IP regulated non-small cell lung cancer (NSCLC) cell malignant phenotypes through miR-5195-3p. (a) Relative levels of miR-5195-3p in NSCLC cell lines with in-miR-NC or in-miR-5195-3p. (b–g) NSCLC cells were transfected with sh-NC, sh-circERBB2IP, sh-circERBB2IP + in-miR-NC, or sh-circERBB2IP + in-miR-5195-3p. (b–f) The proliferation, migration, and invasion of NSCLC cells was determined by 3-(4,5-dimethylthiazol-2-yl)-2,5-diphenyltetrazolium bromide (MTT) (b and c), 5-ethynyl-2′-deoxyuridine () (d), and transwell assays (e and f). (g) Western blotting exhibiting protein levels of E-cad, N-cad, and vimentin protein levels in NSCLC cells. **$p < 0.01$ and ***$p < 0.001$.

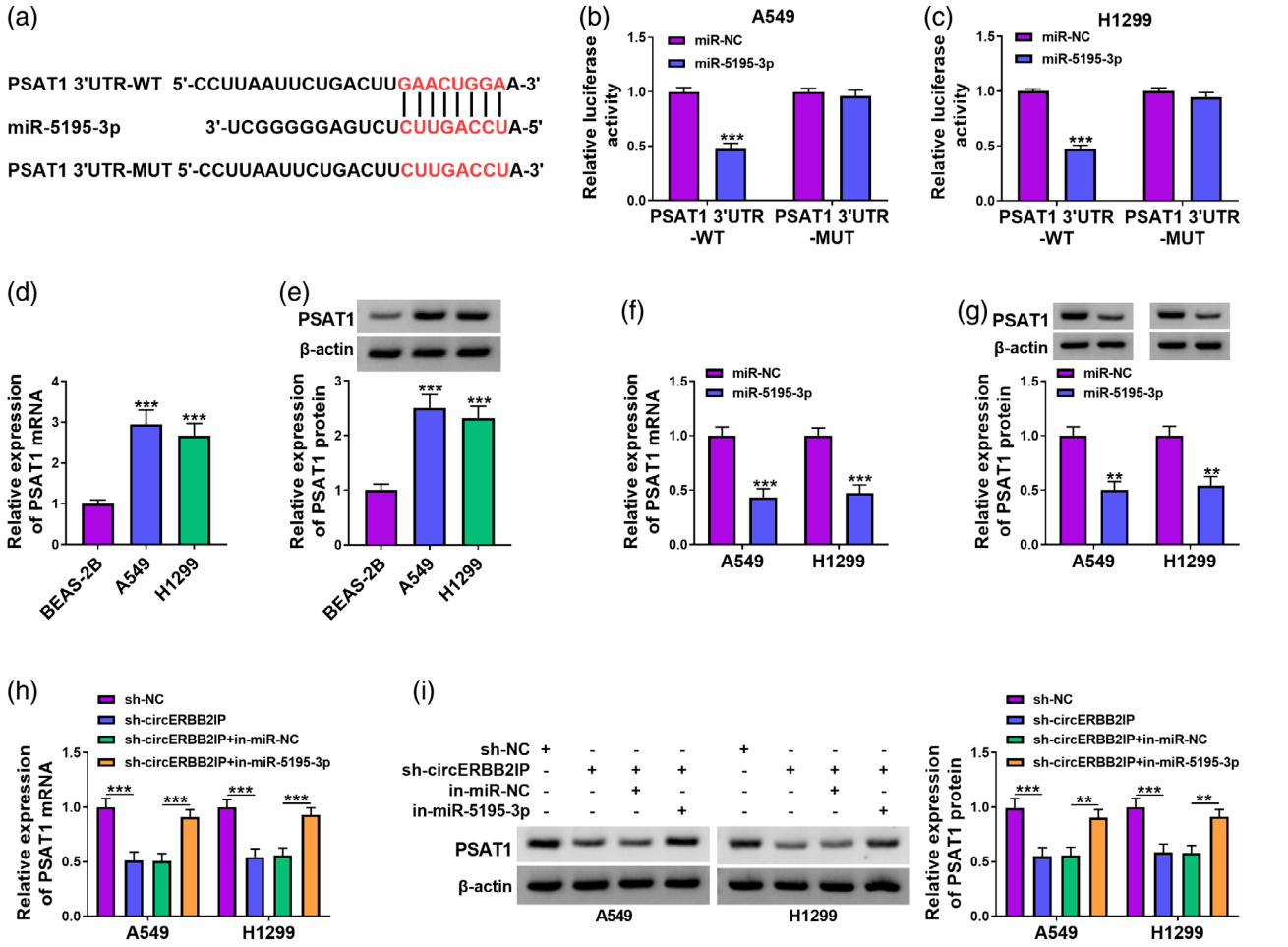

FIGURE 6 PSAT1 was a target of miR-5195-3p. (a) Predicted miR-5195-3p binding sites in the 3'UTR of PSAT1. (b and c) Dual-luciferase reporter assay was conducted to verify the predicted binding sites between PSAT1 and miR-5195-3p. (d) Analysis of PSAT1 mRNA levels in NSCLC samples and normal samples. (e) The correlation between miR-5195-3p and PSAT1 mRNA expression levels in NSCLC samples. (f–k) Analysis of PSAT1 mRNA and protein levels in non-small cell lung cancer (NSCLC) cells (f and g), NSCLC cells with miR-5195-3p mimic or miR-NC (h and i), and NSCLC cells with sh-NC, sh-circERBB2IP, sh-circERBB2IP + in-miR-NC, or sh-circERBB2IP + in-miR-5195-3p (j and k). $^{**}p < 0.01$ and $^{***}p < 0.001$.

DISCUSSION

Exosome-associated RNAs are emerging as key molecules in biomarker development.[28] CircERBB2IP has been discovered as a potential diagnostic marker for the early diagnosis of lung adenocarcinoma.[11] Our data showed higher levels of circERBB2IP in serum-derived exosomes, and the AUC for exosomal circERBB2IP was 0.9168, indicating exosomal circERBB2IP has great potential for diagnosing NSCLC. Communication between carcinoma cells or between carcinoma cells and normal cells through exosomes is essential for tumor growth and metastasis.[29] In the current study, circERBB2IP was also upregulated in NSCLC cells-derived exosomes, and circERBB2IP was delivered in NSCLC cells via exosomes. Functional experiments uncovered the inhibitory effects of circERBB2IP silencing on NSCLC proliferation, migration, invasion, and EMT. Also, circERBB2IP knockdown decreased NSCLC cell proliferation and EMT in vivo. These results illustrated the important role of exosomal circERBB2IP in NSCLC progression.

Some circRNAs act as miRNA sponges in carcinoma cells, leading to inhibition of miRNA expression. Luciferase reporter, RIP, and pulldown assays validated the sponge effect of circERBB2IP on miR-5195-3p. The available evidence suggests that miR-5195-3p exerts an inhibitory activity in a variety of tumors, such as hepatocellular carcinoma,[17] ovarian carcinoma,[30] and bladder carcinoma.[16] Herein, and knocking down circERBB2IP affected miR-5195-3p levels in NSCLC cells. Rescue experiments showed that the circERBB2IP silencing-induced repression on proliferation, migration, invasion, and EMT could be weakened after miR-5195-3p inhibition. Our results support that circERBB2IP binds to miR-5195-3p to mediate NSCLC progression.

PSAT1 was proved as a novel target for miR-5195-3p. Moreover, PSAT1 was overexpressed in NSCLC cells, and upregulated PSAT1 could weaken the inhibiting effects of circERBB2IP downregulation on NSCLC cell malignant phenotypes. Moreover, circERBB2IP could positively regulate PSAT1 expression through binding to miR-5195-3p.

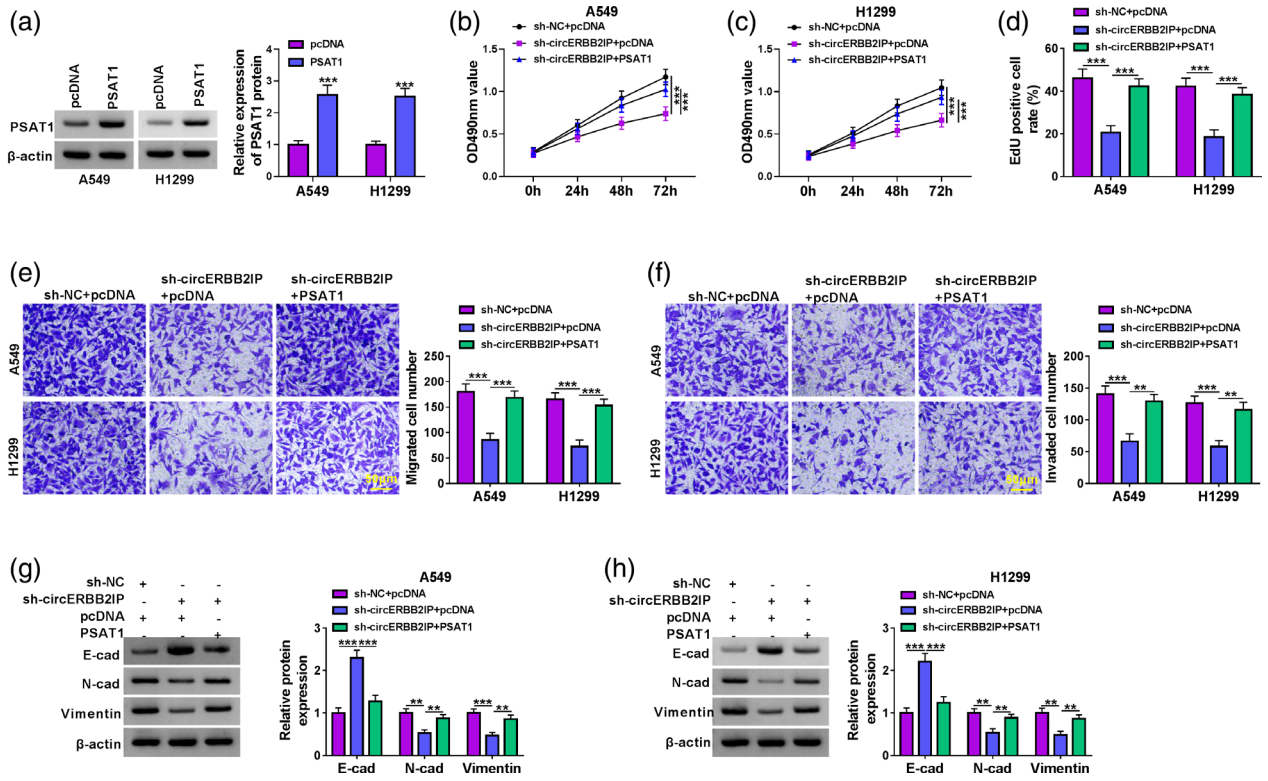

FIGURE 7 CircERBB2IP regulated NSCLC cell malignant phenotypes through positively regulating PSAT1 expression. (a) Western blotting showing PSAT1 protein levels in non-small cell lung cancer (NSCLC) cells with PSAT1 or pcDNA. (b–h) NSCLC cells were transfected with sh-NC, sh-circERBB2IP, sh-circERBB2IP + pcDNA, or sh-circERBB2IP + PSAT1. (b–f) 3-(4,5-dimethylthiazol-2-yl)-2,5-diphenyltetrazolium bromide (MTT), 5-ethynyl-2′-deoxyuridine (EdU), and transwell assays were used to evaluate NSCLC cell proliferation, migration, and invasion. (g and h) Western blotting was used to evaluate E-cad, N-cad, and vimentin protein levels in NSCLC cells. $^{**}p < 0.01$ and $^{***}p < 0.001$.

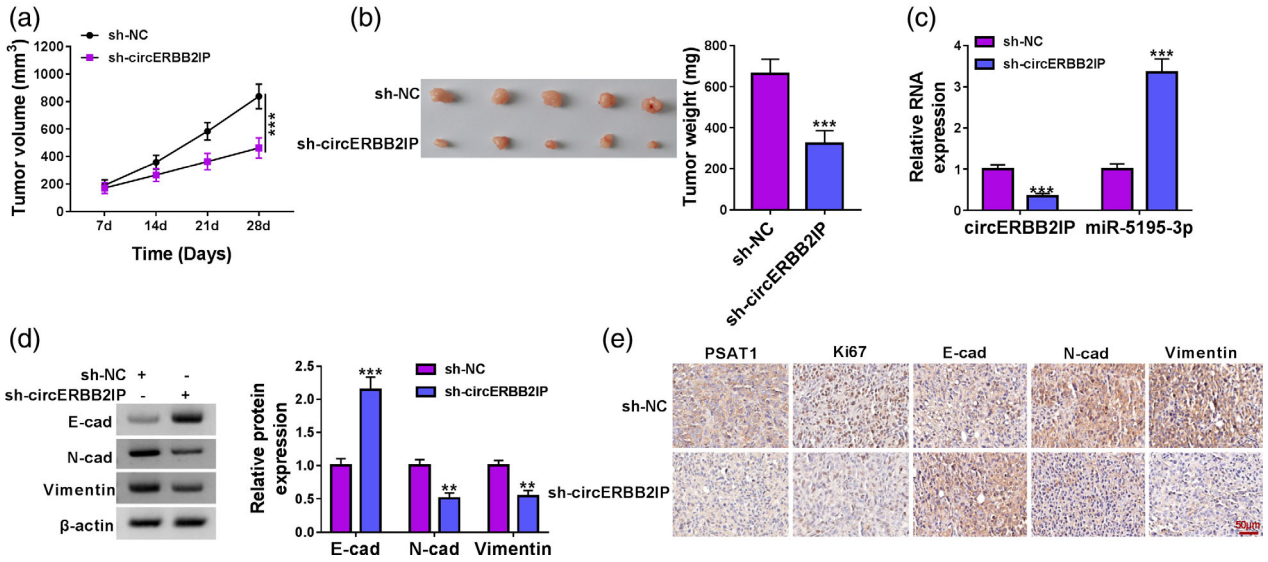

FIGURE 8 CircERBB2IP silencing decreased xenograft tumor growth. (a) Tumor volume in nude mice injected with A549 cells with sh-circERBB2IP or sh-NC. (b) Tumor weight in nude mice injected with A549 cells with sh-circERBB2IP or sh-NC. (c) Relative levels of circERBB2IP and miR-5195-3p in xenograft tumors. (d) Relative protein levels of E-cad, N-cad, and vimentin in xenograft tumors. (e) Immunohistochemistry (IHC) was performed to detect PSAT1, Ki67, E-cad, N-cad, and vimentin expression in xenograft tumors. $^{**}p < 0.01$ and $^{***}p < 0.001$.

Elevated expression of PSAT1 has been observed in a variety of tumor types and is associated with poor clinical outcomes.[27] PSAT1 inhibited the degradation of cyclin D1, thereby changing the activity of the Rb-E2F pathway, leading to the promotion of NSCLC cell proliferation.[25] PSAT1 also contributed to NSCLC cell metastasis through

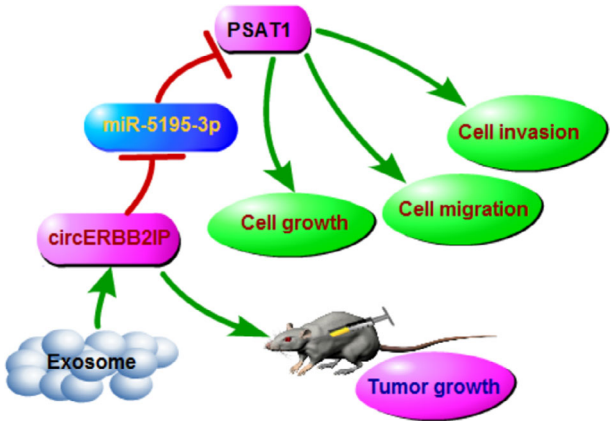

FIGURE 9 Schematic illustration of the circERBB2IP/miR-5195-3p/PSAT1 axis mediating non-small cell lung cancer (NSCLC) progression.

inhibiting the IRF1-IFNγ axis.[24] Accordingly, we concluded that circERBB2IP mediated NSCLC cell malignant phenotypes through PSAT1 via sponging miR-5195-3p.

In conclusion, our study uncovered that serum-derived exosomal circERBB2IP might be a potential diagnostic biomarker for NSCLC. Moreover, circERBB2IP could be transmitted between NSCLC cells through exosomes, and circERBB2IP silencing decreased cell proliferation, migration, invasion, and EMT through downregulating PSAT1 via sponging miR-5195-3p. Thus, we inferred that exosomal circERBB2IP contributed to cell malignant phenotypes and tumor growth through the miR-5195-3p/PSAT1 axis (Figure 9). Our findings expand the understanding of NSCLC progression and shed light on diagnostic biomarkers and therapeutic targets for NSCLC.

AUTHOR CONTRIBUTIONS

Linong Yao designed and performed the research; Jingzhi Dong, Wei Wu, and Tao Luo analyzed the data; Xijuan Peng and Lanfu Zhao wrote the manuscript. All authors read and approved the final manuscript.

ACKNOWLEDGMENTS

None.

CONFLICT OF INTEREST STATEMENT

The authors declare that they have no conflicts of interest.

ORCID

Tao Luo https://orcid.org/0009-0002-3488-5313

REFERENCES

1. Siegel RL, Miller KD. Cancer statistics, 2021. CA Cancer J Clin. 2021;71(1):7–33.
2. Singh SS, Dahal A, Shrestha L, Jois SD. Genotype driven therapy for non-small cell lung cancer: resistance, pan inhibitors and immunotherapy. Curr Med Chem. 2020;27:5274–316.
3. Sun CY, Li YZ, Cao D, Zhou YF, Zhang MY, Wang HY. Rapamycin and trametinib: a rational combination for treatment of NSCLC. Int J Biol Sci. 2021;17:3211–23.
4. Ghafouri-Fard S, Khoshbakht T, Bahranian A, Taheri M, Hallajnejad M. CircMTO1: a circular RNA with roles in the carcinogenesis. Biomed Pharmacother. 2021;142:112025.
5. Liang ZX, Liu HS, Xiong L, Yang X, Wang FW, Zeng ZW, et al. A novel NF-κB regulator encoded by circPLCE1 inhibits colorectal carcinoma progression by promoting RPS3 ubiquitin-dependent degradation. Mol Cancer. 2021;20:103.
6. Rong Z, Shi S, Tan Z, Xu J, Meng Q, Hua J, et al. Circular RNA CircEYA3 induces energy production to promote pancreatic ductal adenocarcinoma progression through the miR-1294/c-Myc axis. Mol Cancer. 2021;20:106.
7. Li C, Zhang L, Meng G, Wang Q, Lv X, Zhang J. Circular RNAs: pivotal molecular regulators and novel diagnostic and prognostic biomarkers in non-small cell lung cancer. J Cancer Res Clin Oncol. 2019;145:2875–89.
8. Liu Z, Wang T, She Y, Wu K, Gu S, Li L, et al. N6-methyladenosine-modified circIGF2BP3 inhibits CD8+ T-cell responses to facilitate tumor immune evasion by promoting the deubiquitination of PD-L1 in non-small cell lung cancer. Mol Cancer. 2021;20:105.
9. Martín J, Castellano JJ, Marrades RM, Canals J, Viñolas N, Díaz T, et al. Role of the epithelial-mesenchymal transition-related circular RNA, circ-10720, in non-small-cell lung cancer. Transl Lung Cancer Res. 2021;10:1804–18.
10. Chen LY, Wang L, Ren YX, Pang Z, Liu Y, Sun XD, et al. The circular RNA circ-ERBIN promotes growth and metastasis of colorectal cancer by miR-125a-5p and miR-138-5p/4EBP-1 mediated cap-independent HIF-1α translation. Mol Cancer. 2020;19:164.
11. Chen F, Huang C, Wu Q, Jiang L, Chen S, Chen L. Circular RNAs expression profiles in plasma exosomes from early-stage lung adenocarcinoma and the potential biomarkers. J Cell Biochem. 2020;121:2525–33.
12. Kok VC, Yu CC. Cancer-derived exosomes: their role in cancer biology and biomarker development. Int J Nanomedicine. 2020;15:8019–36.
13. Mashouri L, Yousefi H, Aref AR, Ahadi AM, Molaei F, Alahari SK. Exosomes: composition, biogenesis, and mechanisms in cancer metastasis and drug resistance. Mol Cancer. 2019;18:75.
14. McAndrews KM, Kalluri R. Mechanisms associated with biogenesis of exosomes in cancer. Mol Cancer. 2019;18:52.
15. Hansen TB, Kjems J, Damgaard CK. Circular RNA and miR-7 in cancer. Cancer Res. 2013;73:5609–12.
16. Jiang Z, Zhang Y, Cao R, Li L, Zhong K, Chen Q, et al. miR-5195-3p inhibits proliferation and invasion of human bladder cancer cells by directly targeting oncogene KLF5. Oncol Res. 2017;25:1081–7.
17. Li Y, Jiang A. ST8SIA6-AS1 promotes hepatocellular carcinoma by absorbing miR-5195-3p to regulate HOXB6. Cancer Biol Ther. 2020;21:647–55.
18. Liu M, Gong C, Xu R, Chen Y, Wang X. MicroRNA-5195-3p enhances the chemosensitivity of triple-negative breast cancer to paclitaxel by downregulating EIF4A2. Hematol Oncol. 2019;24:47.
19. Wang L, Shi G, Zhu D, Jin Y, Yang X. miR-5195-3p suppresses cell proliferation and induces apoptosis by directly targeting NEDD9 in osteosarcoma. Cancer Biother Radiopharm. 2019;34:405–12.
20. Basurko MJ, Marche M, Darriet M, Cassaigne A. Phosphoserine aminotransferase, the second step-catalyzing enzyme for serine biosynthesis. IUBMB Life. 1999;48:525–9.
21. Gao S, Ge A, Xu S, You Z, Ning S, Zhao Y, et al. PSAT1 is regulated by ATF4 and enhances cell proliferation via the GSK3β/β-catenin/cyclin D1 signaling pathway in ER-negative breast cancer. J Exp Clin Cancer Res. 2017;36:179.
22. Zhang Y, Li J, Dong X, Meng D, Zhi X. PSAT1 regulated oxidation-reduction balance affects the growth and prognosis of epithelial ovarian. Cancer. 2020;13:5443–53.
23. Yuan L, Yao L, Wang H. Overexpression of PSAT1 regulated by G9A sustains cell proliferation in colorectal cancer. Onco Targets Ther. 2020;5:47.

24. Chan YC, Chang YC. Overexpression of PSAT1 promotes metastasis of lung adenocarcinoma by suppressing the IRF1-IFNγ axis. Oncogene. 2020;39:2509–22.
25. Yang Y, Wu J, Cai J, He Z, Yuan J, Zhu X, et al. PSAT1 regulates cyclin D1 degradation and sustains proliferation of non-small cell lung cancer cells. Int J Cancer. 2015;136:E39–50.
26. Liang G, Kan S, Zhu Y, Feng S, Feng W, Gao S. Engineered exosome-mediated delivery of functionally active miR-26a and its enhanced suppression effect in HepG2 cells. Int J Nanomedicine. 2018;13:585–99.
27. Biyik-Sit R, Kruer T. Nuclear pyruvate kinase M2 (PKM2) contributes to phosphoserine aminotransferase 1 (PSAT1)-mediated cell migration in EGFR-activated lung cancer cells. 2021;13:3938.
28. Lässer C. Exosomes in diagnostic and therapeutic applications: biomarker, vaccine and RNA interference delivery vehicle. Expert Opin Biol Ther. 2015;15:103–17.
29. Wortzel I, Dror S, Kenific CM, Lyden D. Exosome-mediated metastasis: communication from a distance. Dev Cell. 2019;49:347–60.
30. Ebrahimi SO, Reiisi S. Downregulation of miR-4443 and miR-5195-3p in ovarian cancer tissue contributes to metastasis and tumorigenesis. Arch Gynecol Obstet. 2019;299:1453–8.

SUPPORTING INFORMATION

Additional supporting information can be found online in the Supporting Information section at the end of this article.

How to cite this article: Peng X, Zhao L, Yao L, Dong J, Wu W, Luo T. Exosomal ERBB2IP contributes to tumor growth via elevating PSAT1 expression in non-small cell lung carcinoma. Thorac Cancer. 2023;14(19):1812–23. https://doi.org/10.1111/1759-7714.14926